Optics Communications 445 (2019) 255–261

Contents lists available at ScienceDirect

Optics Communications

journal homepage: www.elsevier.com/locate/optcom

Scintillation index analysis of an optical wave propagating through the moderate-to-strong turbulence in satellite communication links

Xin Shan [a,*], Curtis Menyuk [b], Jing Chen [a], Yong Ai [a]

[a] Electronic Information School, Wuhan University, Wuhan, Hubei, 430072, China
[b] University of Maryland, Baltimore County, Baltimore, MD, 21250, United States

ARTICLE INFO

Keywords:
Scintillation index
Three-layer altitude-dependent turbulence model
Stratospheric turbulence
Optical wave propagation
Laser satellite communication

ABSTRACT

In laser satellite communications, studies of the scintillation index that are based on the three-layer altitude-dependent turbulence model have paid little attention to the different character of stratospheric turbulence from turbulence in the other two layers. This difference is a consequence of the special power spectrum with a power law exponent of 5. By adopting different wave structure functions at different altitudes in the extended Rytov theory, we analyze the scintillation index along the slant path in the regime of moderate-to-strong turbulence. Our results show that the weak fluctuation theory is limited to a smaller zenith angle, and the scintillation index has a larger maximum value in the focusing regime, when compared to the Kolmogorov model. We also find that the change of the scintillation index with the outer scale of the stratospheric turbulence only appears with moderate-to-strong turbulence, and it weakens with the increase of the turbulence outer scale. Moreover, the impact of the Gaussian beam radius on the scintillation index is different in the downlink and the uplink paths. We can approximate the downlink beam as a plane wave in most cases, but we must optimize the uplink beam to minimize the irradiance fluctuation.

1. Introduction

Due to its large bandwidth and good directionality compared to radio frequency transmission, optical transmission with lasers can be used to create a high-speed data link between the ground and satellites. However, the performance of laser communications is affected by signal fading due to intensity scintillation, which is induced by atmospheric turbulence in the optical channel [1,2]. As a result, scintillation must be understood and compensated when establishing a reliable optical communication link.

The Kolmogorov theory, developed in the 1940s, is the most commonly-used model to describe the spatial power spectrum of atmospheric turbulence [1]. Although the Kolmogorov model is widely accepted, numerous works indicate that turbulence in the troposphere and stratosphere obeys non-Kolmogorov statistics [3–5]. In order to take into account variations in the earth's atmosphere with altitude, a two-layer altitude-dependent spectrum was proposed to analyze the impact of the atmospheric turbulence on the scintillation and the star-image motion, in which power laws of tropospheric and stratospheric turbulence spectra are 11/3 and 5, respectively [6,7]. Later, a more accurate three-layer model was developed [8,9]. In this model, the atmosphere near the earth's surface is divided into the boundary layer (up to about 1–2 km), the free troposphere (up to about 8–10 km) and the stratosphere above them, whose turbulence spectrum power law exponents are 11/3, 10/3 and 5, respectively. Based on multi-layer turbulence models, prior works have investigated the propagation characteristics of the optical wave, including the irradiance and the angle-of-arrival fluctuations [8,10,11], and have analyzed the performance of laser satellite communication systems assuming weak turbulence [9,12]. However, it has been found that the Rytov theory can only be applied within a small range of zenith angle (less than 60°) in the slant path propagation [13]. Therefore, it is necessary to study irradiance fluctuation that is influenced by moderate-to-strong turbulence in satellite communications. In Ref. [14], the BER performance was analyzed using the extended Rytov theory assuming weak-to-strong turbulence. However, this work did not take the special characteristics of stratospheric turbulence into consideration. The non-Kolmogorov stratospheric turbulence differs significantly from turbulence in the boundary layer and in the free troposphere, and has a power law exponent that is larger than 4. So the effect of the turbulence outer scale cannot be neglected, especially in the case of moderate-to-strong turbulence [15,16].

In this paper, we focus on the special character of the stratospheric turbulence when the moderate-to-strong fluctuation theory applies. Moreover, we derive the on-axis scintillation index (SI) of the Gaussian optical beam, not just the unbounded laser beam, such as the

* Corresponding author.
E-mail address: sx@whu.edu.cn (X. Shan).

https://doi.org/10.1016/j.optcom.2019.04.052
Received 6 November 2018; Received in revised form 15 March 2019; Accepted 16 April 2019
Available online 20 April 2019

plane wave beam or the spherical wave beam [9,14]. The three-layer altitude-dependent turbulence model is used while presuming that the pointing error is zero. We analyze the influence of the radius of the Gaussian beam on the intensity fluctuation, and the turbulence effect on the intensity fluctuation in the slant optical path of a laser satellite communication system.

The paper is organized as follow. In Section 2, we first present the turbulence power spectrum of the three-layer turbulence model. In Section 3, based on the three-layer model, we develop the theoretical model of the SI, examining both the cases of weak turbulence and moderate-to-strong turbulence. We present our results and discussions in Section 4. Finally, Section 5 contains the conclusion.

2. Three-layer altitude-dependent turbulence model

In the optical link of laser satellite communications, the turbulence spectrum in all three layers can be expressed as [8]

$$\Phi(\kappa,\alpha,h) = A(\alpha_i)\,\beta_i(h)\,\kappa^{-\alpha_i}, \quad i=1,2,3, \tag{1}$$

where α_i is the power law exponent of the turbulence spectrum, κ is the spatial wavenumber, and h is the altitude. The constant $A(\alpha)$ is given by

$$A(\alpha) = \sin\left[(\alpha-3)\pi/2\right]\cdot\Gamma(\alpha-1)/4\pi^2, \quad 3<\alpha<5, \tag{2}$$

where $\Gamma(\bullet)$ is the gamma function. The general refractive index structure constant $\beta(z)$ has units of $m^{3-\alpha}$, which is similar to the refractive index structure parameter C_n^2 in the Kolmogorov model, and is given by

$$\beta(h) = \frac{A(11/3)}{A(\alpha)}C_n^2\left(\frac{k}{L}\right)^{\frac{1}{2}(\alpha-11/3)}, \tag{3}$$

where $k = 2\pi/\lambda$ is the wave number and L is the propagation distance.

In the three-layer turbulence model, the turbulence in the boundary layer obeys Kolmogorov's hypothesis with a power law exponent $\alpha_1 = 11/3$; while turbulence in the free troposphere and stratosphere have non-Kolmogorov turbulence spectra, whose power law exponents are $\alpha_2 = 10/3$ and $\alpha_3 = 5$, respectively. For the stratospheric turbulence, we let $A(\alpha\to5)$ approach 0.0024 in this model [8]. In general, the layer altitudes are free parameters that do not have exact values. For the computational convenience, we assume that the tops of the boundary layer and free troposphere are 2 km and 9 km, respectively.

3. Theoretical model of the scintillation index

In laser satellite communications, the optical wave beam is assumed to be a collimated Gaussian beam. We can use two input-plane beam parameters $\Theta_0 = 1$ and $\Lambda_0 = 2L/kW_0^2$ to characterize it, where W_0 is the beam radius at the transmitter [1]. Analogous to Θ_0 and Λ_0, $\Theta = \Theta_0/(\Theta_0^2+\Lambda_0^2)$ and $\Lambda = \Lambda_0/(\Theta_0^2+\Lambda_0^2)$ are called the output-plane beam parameters. We will concentrate our attention on the SI of the Gaussian beam based on the three-layer turbulence model. We first analyze the case of weak turbulence, and we then extend our analysis to the case of moderate-to-strong turbulence.

3.1. Weak turbulence

In the weak turbulence limit, the log-amplitude variance σ_χ^2 is sufficiently small ($\sigma_\chi^2 \ll 1$), so that the scintillation index σ_I^2 is given by [1]

$$\sigma_I^2 \approx 4\sigma_\chi^2 = 8\pi^2k^2\sec(\zeta)\,\mathrm{Re}\left(\int_{h_0}^{H}\int_0^\infty \kappa\Phi(\kappa)\left\{\exp\left(-\frac{\Lambda L\kappa^2\xi^2}{k}\right)\right.\right.$$
$$\left.\left.-\exp\left[-\frac{iL\kappa^2\xi}{k}\left(1-\left(\bar{\Theta}+i\Lambda\right)\xi\right)\right]\right\}d\kappa\,d\xi\right), \tag{4}$$

where h_0 and H are the ground station altitude and satellite altitude, respectively, ζ is the zenith angle of the optical channel, and Re(•) denotes the real part of the integration. For the downlink path, we have $\xi = (h-h_0)/(H-h_0)$; while for the uplink path, we have $\xi = 1-(h-h_0)/(H-h_0)$.

Substituting the turbulence spectrum of the three-layer model, shown as Eq. (1), into Eq. (4), the SI of the laser beam can be written as

$$\sigma_I^2 = \sum_{i=1}^{3}\sigma_{R\_i}^2 = \sum_{i=1}^{3}4\pi^2A(\alpha_i)\Gamma\left(1-\frac{\alpha_i}{2}\right)k^{3-\frac{\alpha_i}{2}}\sec(\zeta)\,L^{\frac{\alpha_i}{2}-1}\mu_{1\_i}(\Lambda,\Theta,\alpha_i), \tag{5}$$

where $\sigma_{R\_1}^2$, $\sigma_{R\_2}^2$ and $\sigma_{R\_3}^2$ are the scintillation indexes induced by turbulence in the boundary layer, free troposphere and stratosphere, respectively, assuming the weak irradiance fluctuation. In Eq. (5), parameters $\mu_{1\_i}(\Lambda, \Theta, \alpha_i)$ are given by

$$\mu_{1\_i}(\Lambda,\Theta,\alpha) = \mathrm{Re}\left(\int_{h_{0\_i}}^{H_i}\beta_i(h)\left\{\Lambda^{(\alpha_i-2)/2}\xi^{(\alpha_i-2)}\right.\right.$$
$$\left.\left.-\xi^{(\alpha_i-2)/2}\left[\Lambda\xi+i(1-\bar{\Theta}\xi)\right]^{(\alpha_i-2)/2}\right\}dh\right) \quad i=1,2,3. \tag{6}$$

For the first boundary layer, h_{0_1} is equal to h_0, and H_1 is the top of the boundary layer; for the second layer, h_{0_2} and H_2 are the top altitude of the boundary layer and the free troposphere, respectively; while for the third layer, h_{0_3} is the altitude of the top of the free troposphere, and H_3 is equal to H. Because the log-amplitude fluctuation arises from small scale turbulence, the SI is not sensitive to the large scales. Therefore, the outer scale of the stratospheric turbulence can be ignored in the weak fluctuation theory [15].

Fig. 1 shows a comparison of the scintillation index for the Kolmogorov model and the three-layer altitude model when the zenith angle ζ is 0°. The profile model of the structure constant C_n^2 is the H-$V_{5/7}$ model [1]. The results show that the SI with the three-layer model is larger than the one predicted by the traditional Kolmogorov model. It is because that the irradiance fluctuation induced by the free tropospheric turbulence ($\alpha_2 = 10/3$), which is omitted in the traditional model, is more severe than the irradiance fluctuation that is induced by Kolmogorov turbulence [17]. From Fig. 1, we also find that the scintillation indices of different Gaussian beams in the downlink path are almost the same, but they differ greatly for the uplink path. So, in the weak fluctuation regime, it is reasonable to approximate the downlink propagation beam as an unbounded plane wave beam ($\Theta = 1$ and $\Lambda = 0$); however, an uplink SI analysis that is only based on a spherical wave beam ($\Theta = 0$ and $\Lambda = 0$) will not represent accurately the propagation of all optical beams.

3.2. Saturation regime

Regardless of whether the turbulence is Kolmogorov or non-Kolmogorov, the SI always reaches its maximum value in the so-called focusing regime and then decreases toward a value of unity as the turbulence strength increases [18]. So, for the slant path of the laser communication system, the on-axis scintillation index in the saturation regime can be written as

$$\sigma_I^2(L) = 1+32\pi^2k^2(\sec\varsigma)\int_{h_0}^{H}\int_0^\infty \kappa\Phi(\kappa)\sin^2\left[\frac{L\kappa^2}{2k}\xi\left(1-\bar{\Theta}\xi\right)\right]$$
$$\times\exp\left(-\frac{\Lambda L\kappa^2\xi^2}{k}\right)\exp\left\{-\int_0^1 D_s\left[\frac{L\kappa}{k}w(\tau,\xi)\right]d\tau\right\}d\kappa\,dh, \tag{7}$$

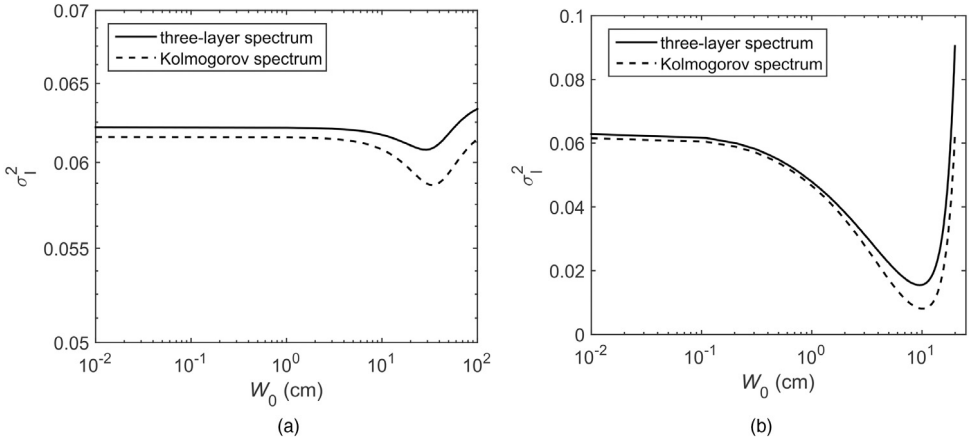

Fig. 1. Scintillation index as a function of W_0 with different models: (a) the downlink optical path, (b) the uplink optical path ($h_0 = 0$ m, $H = 500$ km, and $\lambda = 1550$ nm).

where $D_s(\rho)$ is the plane wave phase structure function, and the parameter $w(\tau, \xi)$ is defined by

$$w(\tau,\xi) = \begin{cases} \tau\left(1-\bar{\Theta}\xi\right), & \tau < \xi \\ \xi\left(1-\bar{\Theta}\tau\right), & \tau > \xi \end{cases}. \tag{8}$$

Based on the geometrical optics approximation, the phase structure function can be approximated by the wave structure function [1]. However, Beland has shown that the wave structure functions are different with different non-Kolmogorov turbulence, which are [16]

$$D_S(\rho,\alpha) = \begin{cases} -2^{4-\alpha}\pi^2 k^2 \rho^{\alpha-2}(\sec\varsigma) A(\alpha) \dfrac{\Gamma\left(1-\frac{\alpha}{2}\right)}{\Gamma\left(\frac{\alpha}{2}\right)}\mu_0, & 2<\alpha<4 \\ 2^2\pi^2 k^2 \rho^2 (\sec\varsigma) A(\alpha) \dfrac{\kappa_0^{4-\alpha}}{(\alpha-2)(\alpha-4)}\mu_0, & \alpha>4 \end{cases} \tag{9}$$

where the parameter μ_0 is given by $\mu_0 = \int_{h_0}^{H} \beta(h)\, dh$, and $\kappa_0 = 2\pi/L_0$, while L_0 is the outer scale of the turbulence. Owing to its special non-Kolmogorov power spectrum, the effect of the outer scale of the stratospheric turbulence must be considered here.

In the three-layer model, atmospheric turbulence exhibits three different characteristics at different altitudes. As was the case in the weak turbulence limit, we can also express the second part of the SI in the saturation regime as a linear superposition of three constituents $\sigma^2_{\ln X\_1}$, $\sigma^2_{\ln X\_2}$ and $\sigma^2_{\ln X\_3}$ at different altitudes, which are given by

$$\begin{aligned} \sigma^2_{\ln X\_i}(L) &= 32\pi^2 k^2 (\sec\varsigma) \int_{h_{0\_i}}^{H_i}\int_0^\infty \kappa \Phi_i(\kappa) \sin^2\left[\frac{L\kappa^2}{2k}\xi\left(1-\bar{\Theta}\xi\right)\right] \\ &\quad \times \exp\left(-\frac{\Lambda L\kappa^2\xi^2}{k}\right) \exp\left\{-\int_0^1 D_{si}\left[\frac{L\kappa}{k}w(\tau,\xi)\right]d\tau\right\} d\kappa dh \\ &\cong 32\pi^2 k^2 (\sec\varsigma) \int_{h_{0\_i}}^{H_i}\int_0^\infty \kappa \Phi_i(\kappa) \left[\frac{L\kappa^2}{2k}\xi\left(1-\bar{\Theta}\xi\right)\right]^2 \\ &\quad \times \exp\left\{-\int_0^1 D_{si}\left[\frac{L\kappa}{k}w(\tau,\xi)\right]d\tau\right\} d\kappa dh, \quad i=1,2,3, \end{aligned} \tag{10}$$

where we have also used the geometrical optics approximation to simplify the result. Therefore, Eq. (10) in the boundary layer and the free troposphere layer has the form

$$\sigma^2_{\ln X\_i}(\alpha_i, L) \cong \frac{\gamma_i(\alpha_i) I_i(\alpha_i)}{\sigma_{R\_i}^{4(4-\alpha_i)/(\alpha_i-2)}}, \quad \sigma^2_{R\_i} \gg 1 \text{ and } i = 1,2, \tag{11}$$

where

$$\gamma_i(\alpha_i) = \frac{2}{\alpha_i - 2}\cdot\frac{1}{\Gamma(1-\alpha_i/2)\cdot\mu_{1\_i}}\cdot\Gamma\left(\frac{6-\alpha_i}{\alpha_i-2}\right)\cdot\left[-\frac{\mu_{0\_i}}{\mu_{1\_i}}\cdot\frac{2^{2-\alpha_i}}{\Gamma(\alpha_i/2)}\right]^{\frac{\alpha_i-6}{\alpha_i-2}} \tag{12a}$$

$$I_i(\alpha_i) = \int_{h_{0\_i}}^{H_i} \beta_i(h)\,\xi^{\alpha_i-4}\left(1-\bar{\Theta}\xi\right)^2 \mu_{11}^{\frac{\alpha_i-6}{\alpha_i-2}} dh \tag{12b}$$

$$\begin{aligned} \mu_{11}\left(\bar{\Theta},\xi,\alpha_i\right) &= \left(1-\bar{\Theta}\xi\right)^{\alpha_i-2}\cdot\frac{\xi}{\alpha_i-1} - \frac{1}{\bar{\Theta}(\alpha_i-1)} \\ &\quad \times\left[\left(1-\bar{\Theta}\right)^{\alpha_i-1} - \left(1-\bar{\Theta}\xi\right)^{\alpha_i-1}\right]. \end{aligned} \tag{12c}$$

In Eq. (12c), $\bar{\Theta}$ cannot be zero; so for the unbounded plane wave, we have $\mu_{11} = 1 + \frac{2-\alpha}{\alpha-1}\xi$.

With the different wave structure function of the stratospheric turbulence, we obtain

$$\sigma^2_{\ln X\_3}(\alpha_3, L) \cong \frac{\gamma_3(\alpha_3) I_3(\alpha_3)}{\sigma_{R\_3}^{4-\alpha_3}}, \quad \sigma^2_{R\_3} \gg 1, \tag{13}$$

where

$$\begin{aligned} \gamma_3(\alpha_3) &= \frac{1}{\Gamma(1-\alpha_3/2)\cdot\mu_{1\_3}}\cdot\Gamma\left(\frac{6-\alpha_3}{2}\right) \\ &\quad \cdot\left[\frac{\mu_{0\_3}}{\mu_{1\_3}}\cdot\frac{1}{\Gamma(1-\alpha_3/2)}\cdot\frac{\kappa_0^{4-\alpha}}{(\alpha_3-2)(\alpha_3-4)}\right]^{\frac{\alpha_3-6}{2}}\left(\frac{k}{L}\right)^{\frac{(\alpha_3-6)(\alpha_3-4)}{4}} \end{aligned} \tag{14a}$$

$$I_3(\alpha_3) = \int_{H_2}^{H} \beta_3(h)\,\xi^{\alpha_3-4}\left(1-\bar{\Theta}\xi\right)^2 \mu_{11}^{\frac{\alpha_3-6}{2}} dh \tag{14b}$$

$$\mu_{11}\left(\bar{\Theta},\xi,\alpha_3\right) = \frac{\xi}{3}\left(1-\bar{\Theta}\xi\right)^2 - \frac{1}{3\bar{\Theta}}\left[\left(1-\bar{\Theta}\right)^3 - \left(1-\bar{\Theta}\xi\right)^3\right] \tag{14c}$$

For the special case of the unbounded plane wave, we find $\mu_{11} = 1 - 2\xi/3$.

3.3. Moderate-to-strong turbulence

For moderate-to-strong turbulence at large zenith angles, the Rytov theory cannot be used because the approximate relation in Eq. (4) is no longer satisfied. However, we can use the extended Rytov theory in which it is assumed that the irradiance field can be expressed as the product of the large-scale turbulence eddy effects, denoted as X, and small-scale effects, denoted as Y. Thus, the scintillation index for strong turbulence can be written as [13]

$$\sigma_I^2 = \exp\left(\sigma^2_{\ln I}\right) - 1 = \exp\left(\sigma^2_{\ln X} + \sigma^2_{\ln Y}\right) - 1. \tag{15}$$

$\sigma^2_{\ln X}$ and $\sigma^2_{\ln Y}$ are the large-scale and small-scale log-irradiance variances, respectively.

If we want to characterize the influence of the various turbulence eddies on the scintillation, the turbulence power-law spectrum has to be modified with a spatial filter, which is represented by [18]

$$G\left(\kappa, l_0, L_0\right) = f\left(\kappa l_0\right) g\left(\kappa L_0\right) \exp\left(-\frac{\kappa^2}{\kappa_X^2}\right) + \frac{\kappa^\alpha}{\left(\kappa^2 + \kappa_Y^2\right)^{\alpha/2}}, \tag{16}$$

where l_0 is the inner scale, κ_X is the large-scale spatial cut-off frequency, and κ_Y is the small-scale spatial cut-off frequency. The first term describe the effects of large-scale turbulence, which includes the inner scale modification factor $f(\kappa l_0)$ and the outer scale modification factor $g(\kappa L_0)$. Here, we ignore the inner scale effect, so that $f(\kappa l_0) = 1$. The outer scale modification factor is

$$g(\kappa L_0) = 1 - \exp(-\kappa^2/\kappa_0'^2), \tag{17}$$

where $\kappa_0' = 8\pi/L_0$. The second term in Eq. (16) is the small-scale spatial filter. Therefore, the large-scale and small-scale log-irradiance variances are given by

$$\begin{aligned}\sigma^2_{\ln X} =& 8\pi^2 k^2 (\sec\varsigma) \int_{h_0}^{H}\int_0^\infty \kappa \Phi(\kappa)\, g(\kappa L_0) \exp\left(-\frac{\kappa^2}{\kappa_X^2}\right) \exp\left(-\frac{\Lambda L \kappa^2 \xi^2}{k}\right) \\ &\times \left(1 - \cos\left[\frac{L\kappa^2}{k}\xi\left(1 - \bar{\Theta}\xi\right)\right]\right) d\kappa dz = \sum_{i=1}^{3} \sigma^2_{\ln X\_i},\end{aligned} \tag{18a}$$

$$\begin{aligned}\sigma^2_{\ln Y} =& 8\pi^2 k^2 (\sec\varsigma) \int_{h_0}^{H}\int_0^\infty \kappa \Phi(\kappa) \frac{\kappa^\alpha}{\left(\kappa^2 + \kappa_Y^2\right)^{\alpha/2}} \exp\left(-\frac{\Lambda L \kappa^2 \xi^2}{k}\right) \\ &\times \left(1 - \cos\left[\frac{L\kappa^2}{k}\xi\left(1 - \bar{\Theta}\xi\right)\right]\right) d\kappa dz = \sum_{i=1}^{3} \sigma^2_{\ln Y\_i},\end{aligned} \tag{18b}$$

where the spatial cut-off frequency of the large-scale and small-scale contributions are [1]

$$\frac{1}{\kappa_X} \approx \begin{cases} \sqrt{L/k}, & \sigma_R^2 \ll 1 \\ L/k\rho_0, & \sigma_R^2 \gg 1 \end{cases} \quad \text{and} \quad \frac{1}{\kappa_Y} \approx \begin{cases} \sqrt{L/k}, & \sigma_R^2 \ll 1 \\ \rho_0, & \sigma_R^2 \gg 1 \end{cases}. \tag{19}$$

$\sigma^2_{\ln X\_i}$ and $\sigma^2_{\ln Y\_i}$ are turbulence-induced large-scale and small-scale log-irradiance variances in three different layers, respectively.

Based on the asymptotic behavior of the SI in the weak and saturation regimes and the superposition of three layers in the slant optical channel, we obtain [18]

$$\sigma_I^2(\alpha) \approx \begin{cases} \sum_{i=1}^{3} \sigma^2_{R\_i} = \sum_{i=1}^{3} (\sigma^2_{\ln X\_i} + \sigma^2_{\ln Y\_i}), & \sigma^2_{R\_i} \ll 1 \\ 1 + 2\sigma^2_{\ln X} = 1 + 2\sum_{i=1}^{3} \sigma^2_{\ln X\_i}, & \sigma^2_{R\_i} \gg 1 \end{cases} \tag{20}$$

where we use the limiting value $\sigma^2_{\ln Y} \longrightarrow \ln 2$ in the saturation regime and assume that $\sigma^2_{\ln Y\_i}$ are same as each other. Therefore, in the boundary layer and the free troposphere of the slant optical channel, the large-scale and small-scale log-irradiance variances are

$$\begin{aligned} &\sigma^2_{\ln X\_i} = 0.49\sigma^2_{R\_i} \quad \text{and} \quad \sigma^2_{\ln Y\_i} = 0.51\sigma^2_{R\_i}, \quad \sigma^2_{R\_i} \ll 1 \\ &\sigma^2_{\ln X\_i} = \frac{\gamma_i(\alpha_i) I_i(\alpha_i)}{2\sigma^{4(4-\alpha_i)/(\alpha_i-2)}_{R\_i}} \quad \text{and} \quad \sigma^2_{\ln Y\_i} = \frac{1}{3}\ln 2, \quad \sigma^2_{R\_i} \gg 1 \end{aligned} \quad i = 1, 2, \tag{21a}$$

while in the stratosphere, they are expressed as

$$\begin{aligned} &\sigma^2_{\ln X\_3} = 0.49\sigma^2_{R\_3} \quad \text{and} \quad \sigma^2_{\ln Y\_3} = 0.51\sigma^2_{R\_3}, \quad \sigma^2_{R\_3} \ll 1 \\ &\sigma^2_{\ln X\_3} = \frac{\gamma_3(\alpha_3) I_3(\alpha_3)}{2\sigma^{4-\alpha_3}_{R\_3}} \quad \text{and} \quad \sigma^2_{\ln Y\_3} = \frac{1}{3}\ln 2, \quad \sigma^2_{R\_3} \gg 1 \end{aligned}. \tag{21b}$$

3.3.1. The boundary layer and the free troposphere

For the boundary layer and the free troposphere turbulence, we neglect the outer scale effects; so $g(\kappa L_0) = 1$. If we define $\eta = L\kappa^2/k, \eta_X = L\kappa_X^2/k, \eta_Y = L\kappa_Y^2/k$, the large-scale log-irradiance variances in these two layers can be written as [18]

$$\begin{aligned}\sigma^2_{\ln X\_i} =& 8\pi^2 k^2 (\sec\varsigma) \int_{h_{0\_i}}^{H_i}\int_0^\infty \kappa \Phi_i(\kappa) \exp\left(-\frac{\kappa^2}{\kappa^2_{X\_i}}\right) \exp\left(-\frac{\Lambda L \kappa^2 \xi^2}{k}\right) \\ &\times \left(1 - \cos\left[\frac{L\kappa^2}{k}\xi\left(1 - \bar{\Theta}\xi\right)\right]\right) d\kappa dz \\ \cong& \frac{\Gamma(3-\alpha_i/2)}{2\Gamma(1-\alpha_i/2)} \cdot \frac{\mu_{2\_i}}{\mu_{1\_i}} \cdot \sigma^2_{R\_i} \cdot \eta_{X\_i}^{3-\frac{\alpha_i}{2}}, \qquad i = 1, 2,\end{aligned} \tag{22a}$$

where we have used the geometrical optics approximation $1 - \cos\left[\left(L\kappa^2/k\right)\xi\left(1 - \bar{\Theta}\xi\right)\right] \cong \left[\left(L\kappa^2/k\right)\xi\left(1 - \bar{\Theta}\xi\right)\right]^2/2$ and $\exp(-\Lambda L\kappa^2\xi^2/k) \cong 1$ to simplify the integral in Eq. (22a). We also have $\mu_{2\_i} = \int_{h_{0\_i}}^{H_i} \beta_i(h)\, \xi^2\left(1 - \bar{\Theta}\xi\right)^2 dh$. The small-scale log-irradiance variances are

$$\begin{aligned}\sigma^2_{\ln Y\_i} =& 8\pi^2 k^2 (\sec\varsigma) \int_{h_{0\_i}}^{H_i}\int_0^\infty \kappa \Phi_i(\kappa) \frac{\kappa^\alpha}{\left(\kappa^2 + \kappa^2_{Y\_i}\right)^{\alpha/2}} \\ &\times \left(1 - \cos\left[\frac{L\kappa^2}{k}\xi\left(1 - \bar{\Theta}\xi\right)\right]\right) d\kappa dh \\ \cong& \frac{-4}{\left(\alpha_i - 2\right)\alpha_i \Gamma(-\alpha_i/2)} \frac{\mu_{0\_i}}{\mu_{1\_i}} \sigma^2_{R\_i} \eta_{Y\_i}^{1-\frac{\alpha_i}{2}}, \qquad i = 1, 2,\end{aligned} \tag{22b}$$

where the cosine term yields the form $\sin\eta/\eta$ at high wave numbers and tends to zero for large η. Considering the asymptotic results of Eq. (19), the spatial cut-off frequencies κ_X^2 and κ_Y^2 can be written as

$$\frac{1}{\kappa_X^2} = C_1(\alpha)\frac{L}{k} + C_2(\alpha)\left(\frac{L}{k\rho_0}\right)^2 \text{ and } \kappa_Y^2 = C_3(\alpha)\frac{k}{L} + C_4(\alpha)\frac{1}{\rho_0^2}. \tag{23}$$

These four scaling constants C_1, C_2, C_3 and C_4 are determined by the asymptotic behavior of Eq. (21). We obtain

$$\eta_{X\_i} \approx \left(0.98\frac{\Gamma(1-\alpha_i/2)}{\Gamma(3-\alpha_i/2)} \cdot \frac{\mu_{1\_i}}{\mu_{2\_i}}\right)^{-\frac{2}{\alpha_i-6}} \cdot \frac{1}{1 + F_{X\_i}(\alpha_i)\sigma^{4/(\alpha_i-2)}_{R\_i}}, \tag{24a}$$

$$\eta_{Y\_i} \approx \left(-0.1275\left(\alpha_i - 2\right)\alpha_i \Gamma(-\alpha_i/2) \cdot \frac{\mu_{1\_i}}{\mu_{0\_i}}\right)^{\frac{2}{2-\alpha_i}} \cdot \frac{1}{1 + F_{Y\_i}(\alpha_i)\sigma^{4/(\alpha_i-2)}_{R\_i}}. \tag{24b}$$

Consequently, the large-scale and small-scale log-irradiance variances are

$$\sigma^2_{\ln X\_i} = \frac{0.49\sigma^2_{R\_i}}{\left(1 + F_{X\_i}(\alpha_i)\sigma^{4/(\alpha_i-2)}_{R\_i}\right)^{3-\alpha_i/2}}, \tag{24c}$$

$$\sigma^2_{\ln Y\_i} = \frac{0.51\sigma^2_{R\_i}}{\left(1 + F_{Y\_i}(\alpha_i)\sigma^{4/(\alpha_i-2)}_{R\_i}\right)^{\alpha_i/2-1}}, \tag{24d}$$

where $F_{X\_i}(\alpha_i) = \left[1.0204\gamma_i\left(\alpha_i\right) I_i\left(\alpha_i\right)\right]^{\frac{2}{\alpha_i-6}}$ and $F_{Y\_i}(\alpha_i) = [0.4530]^{\frac{2}{2-\alpha_i}}$, for $i = 1, 2$.

3.3.2. The stratosphere

Due to the large spectral power law for the stratospheric turbulence in contrast to the other two layer turbulence, its outer scale need to be taken into account in the case of the moderate-to-strong turbulence.

Therefore, the large-scale and small-scale log-irradiance variances become [18]

$$\begin{aligned}\sigma^2_{\ln X\_3} =& 8\pi^2 k^2 (\sec\varsigma) \int_{h_{0\_3}}^{H_3}\int_0^\infty \kappa \Phi_3(\kappa) \exp\left(-\frac{\kappa^2}{\kappa^2_{X\_3}}\right)\left[1 - \exp\left(-\frac{\kappa^2}{\kappa_0'^2}\right)\right] \\ &\times \exp\left(-\frac{\Lambda L \kappa^2 \xi^2}{k}\right)\left(1 - \cos\left[\frac{L\kappa^2}{k}\xi\left(1 - \bar{\Theta}\xi\right)\right]\right) d\kappa dz,\end{aligned} \tag{25a}$$

$$\sigma^2_{\ln Y\_3} = 8\pi^2 k^2 (\sec\varsigma) \int_{h_{0\_3}}^{H} \int_0^{\infty} \kappa \Phi_3(\kappa) \frac{\kappa^{\alpha}}{\left(\kappa^2 + \kappa^2_{Y\_3}\right)^{\alpha/2}} \exp\left(-\frac{\Lambda L \kappa^2 \xi^2}{k}\right) \times \left(1 - \cos\left[\frac{L\kappa^2}{k}\xi\left(1 - \bar{\Theta}\xi\right)\right]\right) d\kappa dz. \tag{25b}$$

The corresponding expressions of the log-irradiance variances and cut-off frequencies are

$$\sigma^2_{\ln X\_3} \cong \frac{\Gamma(3-\alpha_3/2)}{2\Gamma(1-\alpha_3/2)} \cdot \frac{\mu_{2\_3}}{\mu_{1\_3}} \cdot \sigma^2_{R\_3} \cdot \left(\eta^{3-\frac{\alpha_3}{2}}_{X\_3} - \eta^{3-\frac{\alpha_3}{2}}_{X0\_3}\right), \tag{26a}$$

$$\sigma^2_{\ln Y\_3} = \frac{0.51\sigma^2_{R\_3}}{\left(1 + F_{Y\_3}(\alpha_3)\sigma^{4/(\alpha_3-2)}_{R\_3}\right)^{\alpha_3/2-1}}, \tag{26b}$$

$$\eta_{X\_3} \approx \left(0.98\frac{\Gamma(1-\alpha_3/2)}{\Gamma(3-\alpha_3/2)} \cdot \frac{\mu_{1\_3}}{\mu_{2\_3}}\right)^{-\frac{2}{\alpha_3-6}} \cdot \frac{1}{1 + F_{X\_3}(\alpha_3)\sigma^2_{R\_3}}, \tag{26c}$$

$$\eta_{Y\_3} \approx \left(-0.1275\left(\alpha_3 - 2\right)\alpha_3\Gamma(-\alpha_3/2) \cdot \frac{\mu_{1\_3}}{\mu_{0\_3}}\right)^{\frac{2}{2-\alpha_3}} \cdot \frac{1}{1 + F_{Y\_3}(\alpha_3)\sigma^{4/(\alpha_3-2)}_{R\_3}}, \tag{26d}$$

$$\eta_{X0\_3} = \frac{\eta_{X\_3} Q_0}{\eta_{X\_3} + Q_0} \tag{26e}$$

where $F_{X\_3}(\alpha_3) = \left[1.0204\gamma_3\left(\alpha_3\right) I_3\left(\alpha_3\right)\right]^{\frac{2}{\alpha_3-6}}$, $F_{Y\_i}(\alpha_i) = [0.4530]^{\frac{2}{2-\alpha_3}}$ and $Q_0 = L\kappa_0'^2/k = 64\pi^2 L/kL_0^2$.

4. Numerical results and discussion

We investigate the influence of the turbulence on the scintillation index in the Low Earth Orbit (LEO) satellite optical channel. We assume that the altitude of the LEO satellite is 500 km and the ground station is at 0 km. The outer scale of stratospheric turbulence is assumed to be 55 m [10]. In order to concentrate on the difference between the three-layer altitude-dependent model and the traditional Kolmogorov model, we first assume that the laser beam is an unbounded plane wave for the downlink path, while it is a spherical wave for the uplink paths. Fig. 2 shows the comparison results as a function of the zenith angle with a laser wavelength of 1550 nm. In the H-V5/7 model, the upper atmospheric wind speed is 21 m/s, and the turbulence on the ground A is supposed to be on the order of 1.7×10^{-14} $m^{-2/3}$. The zenith angle of the slant path is from 0° to 88°. From these results, we find that, when compared with the Kolmogorov spectrum, the weak fluctuation theory is limited to an even smaller zenith angle based on the three-layer turbulence model. The angle thresholds at which the SI of the strong fluctuation theory begins to diverge from the SI of the weak fluctuation theory are different in both the three-layer turbulence model and the Kolmogorov model. In the former model, the thresholds are around 50° and 60° in the downlink path and the uplink path, respectively; while in the latter model, they are about 60° and 75° respectively. In the strong fluctuation theory, the large-scale scintillation of the plane wave and the spherical wave are quite different [13]. So, the SI of the plane wave increases more slowly when the turbulence increases gradually, leading to a smaller angle threshold for the downlink. Moreover, in the weak fluctuation regime (zenith angle less than 50°), the SI difference between these two turbulence models is very small. However, in the moderate-to-strong turbulence, it becomes larger. The reason is that non-Kolmogorov turbulence, which is included in the three-layer turbulence model, influences the laser beam differently from Kolmogorov turbulence. For non-Kolmogorov turbulence with a power law exponent that is less than 11/3, the maximum SI in the focusing regime is larger than that for Kolmogorov turbulence [19], so that the SI with the three-layer turbulence model has a larger peak value than the SI with Kolmogorov model in the slant path.

In the three-layer turbulence model, the stratospheric turbulence is unique compared to the other two layers due to its special wave structure function, which is affected by the turbulence outer scale and is important in the strong fluctuation theory. Fig. 3 illustrates the impact of the turbulence outer scale on the SI in the downlink and uplink paths using the moderate-to-strong fluctuation theory. The outer scale of the stratosphere turbulence L_0 are assumed to be 55 m, 100 m and 200 m, respectively. When the turbulence becomes stronger, the scintillation index cannot increase without bound. It will reach its maximum value (larger than 1) in what we refer to as the focusing regime. According to the strong fluctuation theory, the focusing effect will be weakened because the spatial coherence is reduced when the turbulence increases continuously (at larger zenith angle), so that the scintillation index decreases gradually. The turnover of the SI curve in the strong fluctuation theory can be also observed in Fig. 2. Results also indicate that the influence of the turbulence outer scale is negligible in the weak fluctuation regime, while SI has a smaller peak value with the larger outer scale in moderate-to-strong turbulence. As a consequence, the range of the zenith angles for which the weak fluctuation theory can be applied decreases gradually. However, as the outer scale continues to increase, its impact on the intensity scintillation diminishes slowly. Moreover, compared with the downlink path, the intensity fluctuation in the uplink path is more severe. This difference of the scintillation index becomes greater when increasing the zenith angle. In particular, when the zenith angle exceeds 80°, the uplink scintillation index is larger than the downlink index by more than 100%.

As we mentioned previously, in the weak fluctuation regime with the three-layer turbulence model, the laser beam can be assumed to be a plane wave beam in the downlink path of the satellite communication. This approximation is still valid under most conditions with moderate-to-strong turbulence. As we showed in Fig. 4(a), only when the zenith angle becomes equal to 85°, the SI decreases significantly when the effective beam radius W_0 is larger than 100 cm. However, in the uplink path, there is always an optimal beam radius, which has the smallest SI no matter how strong the turbulence becomes. When the turbulence continues to increase with a larger zenith angle, this optimal radius becomes larger, which can be seen from Fig. 4(b). The result reveals that the radius of the Gaussian beam has a different influence on the scintillation index for the downlink and uplink paths in laser satellite communication systems.

We also studied the influence of the ground turbulence and the laser wavelength on the scintillation index in a laser satellite communication link that is based on the three-layer altitude-dependent turbulence model. The results are shown in Figs. 5 and 6. The outer scale of the stratosphere turbulence equals 55 m. We find that the turbulence level near the ground and the wavelength both affect the SI. For shorter wavelengths and stronger ground turbulence, the weak turbulence theory is restricted to smaller zenith angles and the maximum SI is smaller, which also happens with the Kolmogorov model [13].

5. Conclusion

In this paper, we theoretically analyzed the on-axis scintillation index in the downlink and uplink paths of the LEO laser satellite communication link. Based on the three-layer altitude-dependent turbulence model, the influence of the special wave structure function of the stratospheric turbulence ($\alpha = 5$) has been taken into the consideration in the moderate-to-strong fluctuation theory, which previous studies of the scintillation index in the slant path have neglected.

The results show the difference in the SI with the three-layer turbulence model and the traditional Kolmogorov model. Due to non-Kolmogorov turbulence in the three-layer turbulence model, the weak turbulence theory can only be applied in a smaller range of zenith angles, and the peak value of the SI in the focusing regime is much larger than the one predicted by the traditional model. The outer scale of the stratospheric turbulence influences the intensity scintillation in the laser satellite communication link when moderate-to-strong turbulence is present. However, its impact would decrease gradually with

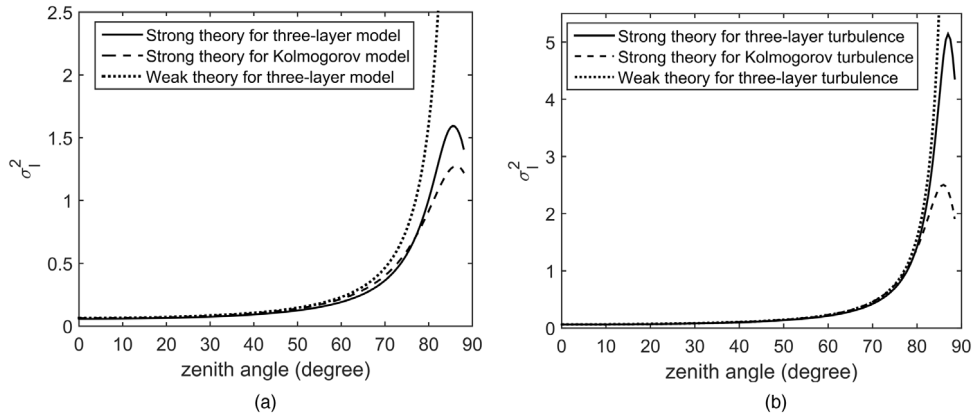

Fig. 2. Scintillation index as a function of the zenith angle with different models: (a) the plane wave beam for the downlink optical path, (b) the spherical wave beam for the uplink optical path.

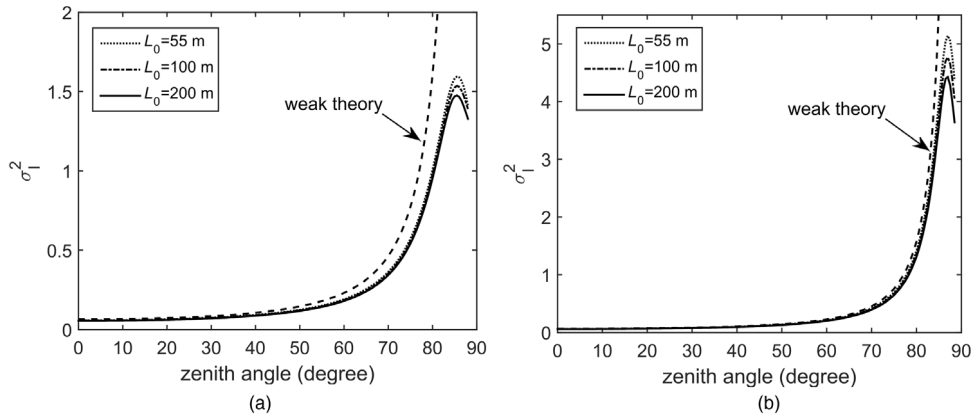

Fig. 3. Scintillation index as a function of the zenith angle and three different outer scales of the stratosphere turbulence with the three-layer turbulence model: (a) the plane wave beam for the downlink optical path, (b) the spherical wave beam for the uplink optical path. ($A = 1.7\times10^{-14}$ m$^{-2/3}$ and $\lambda = 1550$ nm).

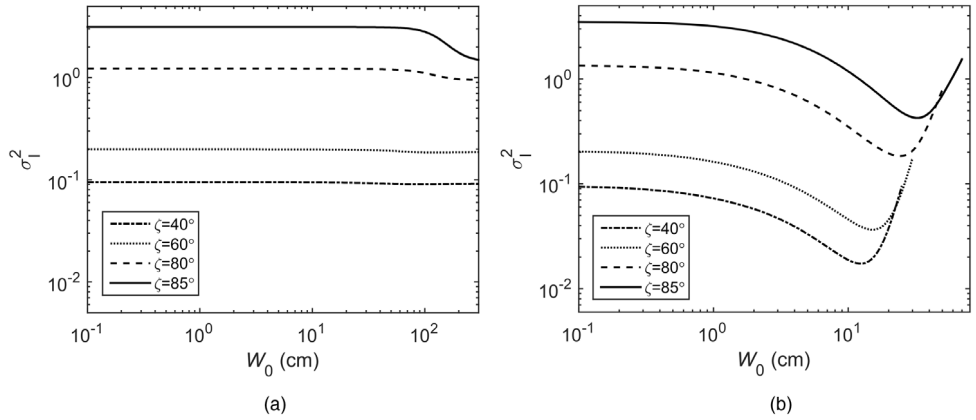

Fig. 4. Scintillation index as a function of W_0 and four different zenith angles with the three-layer turbulence model: (a) the downlink optical path, (b) the uplink optical path. ($A = 1.7\times10^{-14}$ m$^{-2/3}$, $\lambda = 1550$ nm and $L_0 = 50$ m).

the increase of the turbulence outer scale. We also study the effect of the Gaussian laser beam radius, the ground turbulence level, and the laser wavelength in the moderate-to-strong fluctuation theory. In the downlink path, the SI experiences little change with different beam radius in most cases. The SI difference only appears at very large zenith angles. However, in the uplink path, the influence of the beam radius on the scintillation is more significant. Regardless of the zenith angle, there is always an optimal beam radius, which has the smallest SI. Therefore, in a laser satellite communication link, it is reasonable to approximate the laser beam as an unbounded plane wave in the downlink path, but it is better to design an optimal Gaussian beam to mitigate the intensity scintillation in the uplink path.

Acknowledgments

This work was supported by the National Natural Science Foundation of China (Grant No. 11204220), the Shanghai Aerospace Science and Technology Innovation Fund, China (Grant No. SAST2017-103) and China Scholarship Council.

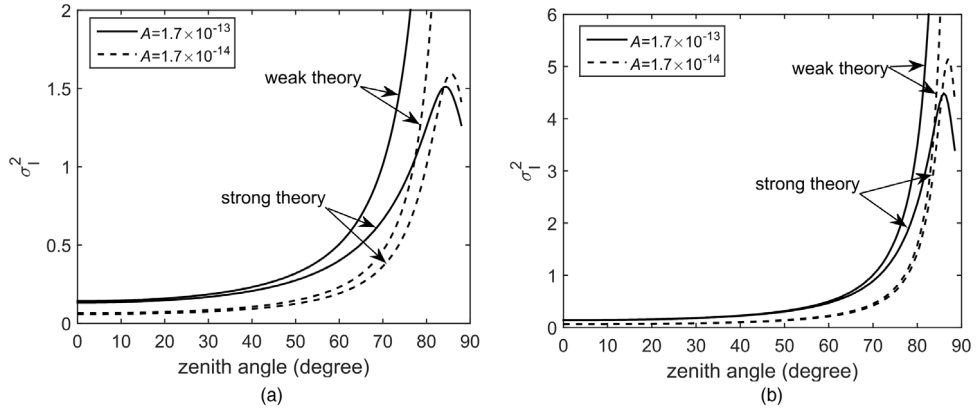

Fig. 5. Scintillation index as a function of the zenith angle and two different ground turbulence levels with the three-layer turbulence model: (a) the plane wave beam for the downlink optical path, (b) the spherical wave beam for the uplink optical path. (λ = 1550 nm).

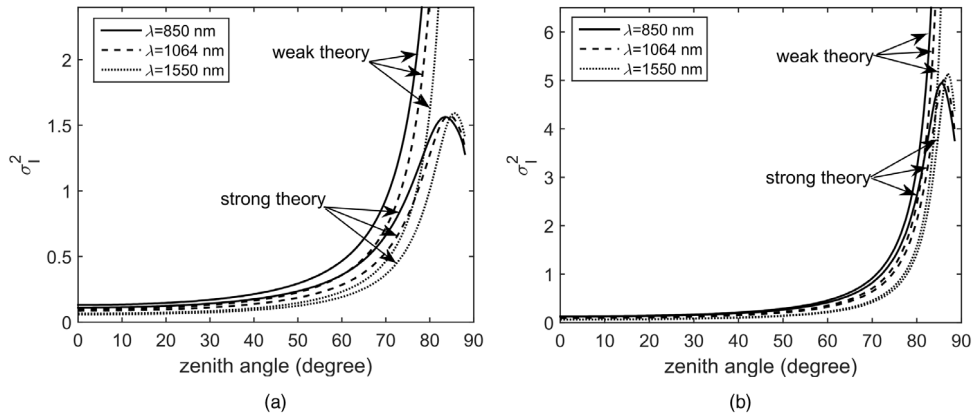

Fig. 6. Scintillation index as a function of the zenith angle and three different laser wavelengths with the three-layer turbulence model: (a) the plane wave beam for the downlink optical path, (b) the spherical wave beam for the uplink optical path. ($A = 1.7\times10^{-14}$ $m^{-2/3}$).

References

[1] L.C. Andrews, R.L. Phillips, Laser Beam Propagation Through Random Media, second ed., SPIE Press, Bellingham, Washington, 2005.

[2] S. Avramov-Zamurovic, C. Nelson, S. Guth, O. Korotkova, R. Malek-Madani, Experimental study of electromagnetic Bessel-Gaussian Schell model beams propagating in a turbulent channel, Opt. Commun. 359 (2016) 207–215.

[3] A. Zilberman, E. Golbralkh, N.S. Kopeika, A. Virtser, I. Kupershmidt, Y. Shtemler, LIDAR study of aerosol turbulence characteristics in the troposphere: Kolmogorov and non-Kolmogorov turbulence, Atmos. Res. 88 (1) (2008) 66–77.

[4] C. Robert, J.M. Conan, V. Michau, J.B. Renard, C. Robert, F. Dalaudier, Retrieving parameters of the anisotropic refractive index fluctuations spectrum in the stratosphere from balloon-borne observations of stellar scintillation, J. Opt. Soc. Amer. A 25 (2) (2008) 379–393.

[5] I. Toselli, Introducing the concept of anisotropy at different scales for modeling optical turbulence, J. Opt. Soc. Amer. A 31 (8) (2014) 1868–1875.

[6] A.S. Gurvich, M.S. Beln'kii, Influence of stratospheric turbulence on infrared imaging, J. Opt. Soc. Amer. A 12 (11) (1995) 2517–2522.

[7] M.S. Beln'kii, Effect of the stratosphere on star image motion, Opt. Lett. 20 (12) (1995) 1359–1361.

[8] A. Zilberman, E. Golbraikh, N.S. Kopeika, Propagation of electromagnetic waves in Kolmogorov and non-Kolmogorov atmospheric turbulence: three-layer altitude model, Appl. Opt. 47 (34) (2008) 6385–6391.

[9] A. Zilberman, E. Golbraikh, N.S. Kopeika, Some limitations on optical communication reliability through Kolmogorov and non-Kolmogorov turbulence, Opt. Commun. 283 (2010) 1229–1235.

[10] S. Fu, L. Tan, J. Ma, Y.P. Zhou, Effect of Non-Kolmogorov turbulence on angle-of-arrival fluctuations of starlight, J. Russ. Laser Res. 31 (4) (2010) 332–337.

[11] W. Du, Z. Yao, D. Liu, C. Cai, X. Du, R. Ai, Influence of non-kolmogorov turbulence on intensity fluctuations in laser satellite communication, J. Russ. Laser Res. 33 (1) (2012) 90–97.

[12] X. Yi, Z. Liu, P. Yue, Uplink laser satellite-communication system performance for a Gaussian beam propagating through three-layer altitude spectrum of weak-turbulence, Optik 124 (2013) 2916–2919.

[13] L.C. Andrews, R.L. Phillips, C.Y. Hopen, Scintillation model for a satellite communication link at large zenith angles, Opt. Eng. 39 (12) (2000) 3271–3280.

[14] P. Yue, L. Wu, X. Yi, Z. Fu, Performance analysis of a laser satellite-communication system with a three-layer altitude spectrum over weak-to-strong turbulence, Optik 148 (2017) 283–292.

[15] R.R. Beland, Some aspects of propagation through weak isotropic non-Kolmogorov turbulence, Proc. SPIE 2375 (1995) 6–16.

[16] C. Rao, W. Jiang, N. Ling, Spatial and temporal characterization of phase fluctuations in non-Kolmogorov atmospheric turbulence, J. Mod. Opt. 47 (6) (2000) 1111–1126.

[17] X. Shan, M. Liu, N. Zhang, Y. Ai, Laboratory simulation of non-Kolmogorov turbulence based on a liquid crystal spatial light modulator, Opt. Eng. 56 (2) (2017) 026111.

[18] L.C. Andrews, R.L. Phillips, C.Y. Hopen, Laser Beam Scintillation with Applicants, SPIE Press, Bellingham, Washington, 2001.

[19] L. Cui, B. Xue, S. Zheng, W. Xue, X. Bai, X. Cao, F. Zhou, Atmospheric spectral model and theoretical expressions of irradiance scintillation index for optical wave propagating through moderate-to-strong non-Kolmogorov turbulence, J. Opt. Soc. Amer. A 29 (6) (2012) 1091–1098.